Characteristics of Shear Damage for 60Sn-40Pb Solder Material*

H. Eliot Fang
Sandia National Laboratories
P.O. Box 5800, MS 0820
Albuquerque, NM 87185-0820, USA

C. L. Chow and Y. Wei
Department of Mechanical Engineering
University of Michigan-Dearborn
Dearborn, MI 48128-1491, USA

Summary

This paper presents an investigation of the development of a continuum damage model capable of accurately analyzing shear damage in 60Sn-40Pb solder material. Based on the theory of damage mechanics, an internal state variable known as the damage variable is introduced to characterize material degradation caused by the change of material microstructures under load. A damage surface in stress space is proposed to quantify damage initiation and its successive expanding surfaces to represent damage hardening. With the aid of irreversible thermodynamics, the damage-coupled constitutive equations and the damage evolution equations are established. A failure criterion is proposed based on the accumulation of overall damage in the material.

The damage model is implemented in a general purpose finite element program ABAQUS through its user-defined material subroutine UMAT. The program is applied to predict shear deformation in a notched specimen. The predicted failure mode and maximum load agree well with those measured experimentally. The effect of finite element meshing on the numerical results is also examined and discussed.

Introduction

The Pb-Sn eutectic alloy is widely used as a joining material in the electronic industry. In this application the solder acts as both electrical and mechanical connection within and among different packaging levels in an electronic device. This application raises concerns on the reliability of solder joints subjected to thermomechanical loading [1-5].

The conventional mechanics approach assumes that all materials are perfect or defect-free. However, real-life materials do contain defects in the form of micro-cracks/voids which will initiate, grow and coalesce under load. The accumulation of damage is manifested as a reduction in the effective load bearing area of solder joints, leading to stiffness degradation or material deterioration which in turns causes macro-crack initiation and eventual rupture. The primary objective of this paper is to present a damage model which can take into account the effects of damage accumulation in solder joints. The methodology is based on the emerging theory of Damage Mechanics. The theory enables a macroscopic description of successive physical deterioration phenomena by introducing a set of internal state variables as a measure of damage in a macroscopically volume average element [6]. Due to thermal mismatch between the materials in the electronic package, solder joints often fail under shear. Therefore, this investigation is intended to provide a validation analysis of the proposed damage model for shear induced damage and failure in 60Sn-40Pb solder material.

DISCLAIMER

DISCLAIMER

Portions of this document may be illegible in electronic image products. Images are produced from the best available original document.

Constitutive Modeling

During a loading process the microstructure of a material changes due to nucleation and growth of micro-cracks or defects. An internal state variable **D** is introduced to describe the gradual deterioration of the material. Based on the concept of damage mechanics, an effective stress $\overline{\sigma}$ is defined as

$$\overline{\sigma} = \mathbf{M(D)}:\sigma \tag{1}$$

where σ is the true stress tensor and **M(D)** is the damage effect tensor. The damage effect tensor may be established as [6]

$$[M_{ij}(D)] = \frac{1}{1-d}\begin{bmatrix} 1 & \mu & \mu & 0 & 0 & 0 \\ \mu & 1 & \mu & 0 & 0 & 0 \\ \mu & \mu & 1 & 0 & 0 & 0 \\ 0 & 0 & 0 & 1-\mu & 0 & 0 \\ 0 & 0 & 0 & 0 & 1-\mu & 0 \\ 0 & 0 & 0 & 0 & 0 & 1-\mu \end{bmatrix} \tag{2}$$

where d and μ are two independent components of damage tensor **D**. Obviously, this damage effect tensor reduces to the typical form $\mathbf{M} = \mathbf{I}/(1-d)$ when the value of μ is assumed to be zero. This corresponds to a special case of isotropic damage for which the value of Poisson's ratio remains constant under load.

According to the hypothesis of energy equivalence [7], the elastic energy for a damaged material is the same as that of the undamaged material when the stress tensor is replaced by its effective stress counterpart in the stress-based form. Mathematically it is expressed as

$$W^e(\sigma,\mathbf{D}) = \frac{1}{2}\overline{\sigma}^T:\mathbf{C}^{-1}:\overline{\sigma} = \frac{1}{2}\sigma^T:\overline{\mathbf{C}}^{-1}:\sigma \tag{3}$$

where W^e is the elastic energy, $\mathbf{C}^{-1}$ is the elastic tensor for undamaged material, and $\overline{\mathbf{C}}^{-1}$ is the effective elastic tensor for damaged material. Therefore, the constitutive equation of elasticity coupled with damage can be derived in the true stress-true strain space by the thermodynamic theory as

$$\varepsilon^e = \frac{\partial W^e(\sigma,\mathbf{D})}{\partial\sigma} = \overline{\mathbf{C}}^{-1} : \sigma \tag{4}$$

For an isotropic material, using Eqs. (1) and (2) and assuming a Von Mises yield criterion, the yield surface of damaged material is expressed as

$$F_p(\sigma, \mathbf{D}, R) = \frac{1-\mu}{1-d}\sigma_{eq} - [R_0 + R(p)] = 0 \tag{5}$$

where σ_{eq} is Von Mises' stress, R_0 is the initial strain hardening threshold, p is the effective equivalent plastic strain, and R is the increment of strain hardening threshold. Similar to the conventional theory of plasticity,

which assumes an associated flow rule, the damage-coupled constitutive plastic equations are derived in the true stress-true strain space as

$$d\varepsilon^p = \lambda_p \frac{\partial F_p}{\partial \sigma} = \frac{1-\mu}{1-d}\frac{3S}{2\sigma_{eq}}\lambda_p \qquad dp = \lambda_p \frac{\partial F_p}{\partial(-R)} = \lambda_p \tag{6}$$

where ε^p is the plastic strain tensor, **S** is the stress deviator tensor and λ_p is a Lagrange multiplier.

The thermodynamic conjugate forces of the plastic damage variables d and μ, known as plastic damage energy release rates, are defined by

$$Y_d = -\frac{\partial W^e}{\partial d} \qquad Y_\mu = -\frac{\partial W^e}{\partial \mu} \tag{7}$$

Then the plastic damage surface is formulated in terms of the plastic damage energy release rate as

$$F_{pd}(Y,B) = Y_{pd}^{1/2} - [B_0 + B(w)] = 0 \qquad Y_{pd} = \frac{1}{2}(Y_d^2 + \gamma Y_\mu^2) \tag{8}$$

where B_0 is the initial plastic damage threshold, B is the plastic damage hardening, w is the overall plastic damage and γ is the damage evolution coefficient. In a similar way as that leading to plastic constitutive equations, the plastic damage evolution laws are derived as

$$\dot{d} = -\lambda_d \frac{\partial F_{pd}}{\partial Y_d} = -\frac{\lambda_d Y_d}{2Y_{pd}^{1/2}} \qquad \dot{\mu} = -\lambda_d \frac{\partial F_{pd}}{\partial Y_\mu} = -\frac{\lambda_d \gamma Y_\mu}{2Y_{pd}^{1/2}} \qquad \dot{w} = \lambda_d \frac{\partial F_{pd}}{\partial(-B)} = \lambda_d \tag{9}$$

Therefore, the plastic damage accumulation under load can be evaluated with Eq. (9). The plastic damage accumulation is used to develop a failure criterion, postulating that a material element is said to have ruptured when the total overall damage w in the element reaches a critical value w_c. The critical value is considered an intrinsic material property which is measured at the rupture strain of a unaxial tensile specimen using the following equation

$$w_c = \sum_i \{2[(\Delta d)_i^2 + \frac{(\Delta\mu)_i^2}{\gamma}]\}^{1/2} \tag{10}$$

where Δd and $\Delta\mu$ are determined respectively from the change of Young's modulus and Poisson's ratio.

Numerical Procedure

Due to damage accumulation, local rigidity in a material element decreases under load. This causes stress/strain redistribution as the damage model changes material properties in one location and then another in a structure through its distributed formulation of constitutive elastic and plastic equations. Such an important facility is unfortunately unavailable in the conventional analysis, to achieve an accurate assessment of structural responses, especially around notches or cracks where the observed damages are pronounced.

Although the constitutive formulations of damaged material are more complex than that of conventional isotropic elasto-plasticity models, the existing finite element analysis can be conveniently modified to include the effects of damage. The modification requires the need to conduct an iteration procedure using the Newton's method in the effective stress/effective strain space for the solution of incremental equivalent effective plastic strain. A new material stiffness matrix can be formed to include the effects of damage accumulation. The damage model has been implemented in a general purpose finite element program ABAQUS through its user-defined material subroutine UMAT.

The overall plastic damage accumulation at each integration point is calculated by the finite element analysis. When its value reaches a critical state w_c, this material point is said to be fully damaged, and the stiffness and stress at that point are set to zero. The failure criterion is applicable to both crack initiation and propagation as a form of unified approach which would not otherwise be possible based on the conventional methods of analysis without damage considerations.

Application

The geometry of a specimen chosen to simulate shear failure is depicted in Fig. 1. The material is commercially available 60Sn-40Pb solder. The strain hardening curve R(p) and the plastic damage hardening rate curve dB/dw at strain rate 10^{-3}/s and room temperature (22°C) are tabulated in Table 1 and 2. Other damage parameters for the material are:

$R_0 = 25.9$ MPa $B_0 = 0.0297$ MPa $\gamma = -0.337$ $w_c = 0.58$

Table 1. Strain Hardening Data.

R_0+R(MPa)	25.9	27.5	29.5	32.6	36.2	40.6	45.1	49.7	54.8
p	0	0.0055	0.025	0.071	0.169	0.322	0.523	0.764	1.088

Table 2. Damage Hardening Rate Data.

dB/dw(MPa)	0.193	0.200	0.242	0.352	0.504	0.690	0.918	1.180	1.490	1.697
w	0.055	0.124	0.228	0.335	0.408	0.464	0.505	0.534	0.556	0.58

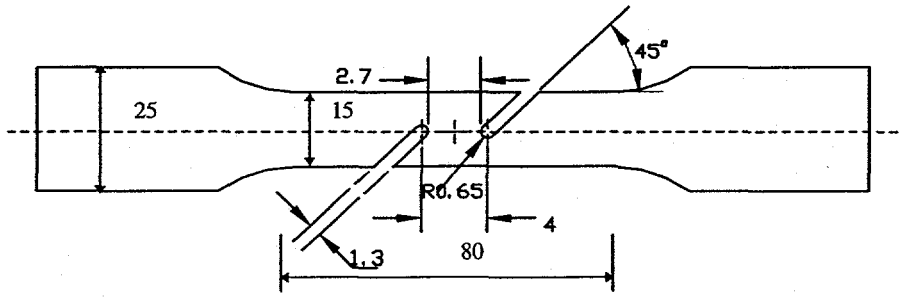

Fig. 1. Specimen Configurations (all unit: mm).

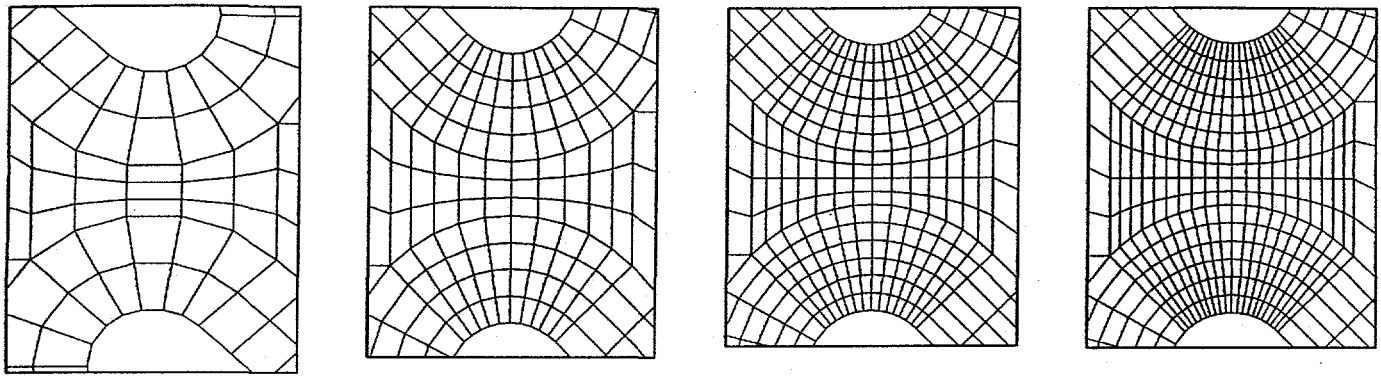

Fig. 2. Different Meshes around the Notches.

There are two layers of elements in the thickness direction. Only one layer of elements is analyzed due to the symmetry of the geometry and the loading condition. The load is applied through the displacement boundary condition. Four different mesh types shown in Fig. 2 around the notches are chosen to examine the effects of mesh size on the numerical solution in the simulation of shear deformation and fracture load.

Both linear, full-integration (C3D8) and reduced-integration (C3D8R) solid elements are used. The predicted maximum loads by the four different meshing types and integration types are shown in Table 3 together with the measured result. It can be observed from Table 3 that a convergent numerical result can be attained with a finer mesh size.

Table 3. Maximum load (lbs).

integration type	numerical result				measured result
	mesh one	mesh two	mesh three	mesh four	
C3D8R	48.3	43.2	39.8	39.7	38.4
C3D8	38.1	37.7	37.4	37.4	

The numerical analysis also reveals that a convergent numerical solution by the linear, full-integration (C3D8) elements can be more readily achieved than by the linear, reduced-integration (C3D8R) elements. But the full-integration elements subjected to bending load may result in inaccurate simulation due to shear locking, as elucidated by the ABAQUS/STANDARD manual. In addition, it is more efficient to simulate crack propagation by C3D8R elements than by those of C3D8. Therefore, a fine mesh of linear, reduced-integration elements is recommended for numerical simulations involving large mesh distortions or crack propagation analysis.

The deformed mesh at the maximum load is shown in Fig. 3. A shear deformation dominated region appears between the two notches. Fig. 4 depicts overall plastic damage accumulation close to the maximum load. It can be readily observed from the figure that a single crack emerges at the notch area along the loading direction. The simulated deformation and fracture patterns coincide with those observed experimentally as depicted in Fig. 5.

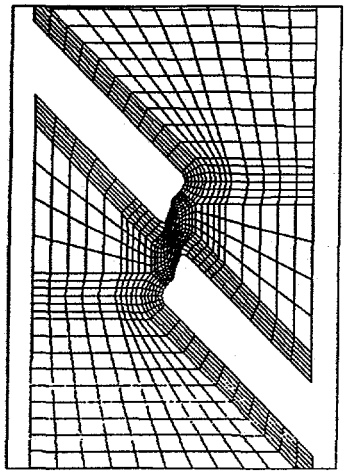

Fig. 3. Deformed Mesh.

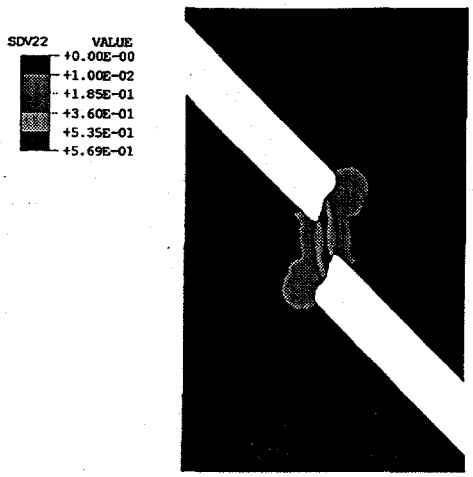

Fig. 4. Contours of Overall Damage.

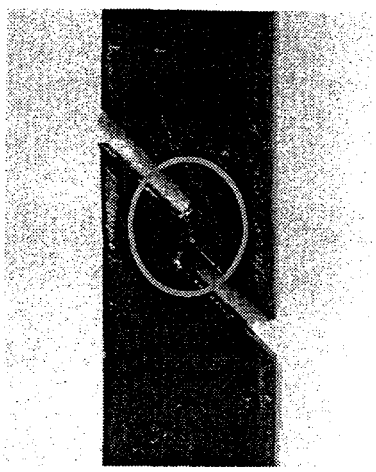

Fig. 5. Test Specimen.

Conclusions

A damage model has been developed and applied successfully to characterize shear deformation of 60Sn-40Pb solder material. The solution is achieved using ABAQUS (version 5.6) through its user-defined subroutine UMAT. Similar deformation and fracture patterns of a notched specimen can be observed from both numerical simulation and experimental tests. The maximum load predicted agrees well with the measured result. A numerical experimentation also reveals that there is a definite effect of mesh size on the accuracy of the solution with finer mesh size yielding a more accurate solution. In addition, a convergent numerical solution using the linear, full-integration (C3D8) elements can be more readily achieved than by using the linear, reduced-integrated (C3D8R) elements.

References

1. Busso, E. P., Kitano, M. and Kumazawa, T, (1994), "Modeling Complex Inelastic Deformation Processes in IC Packages' Solder Joints", Journal of Electronic Packaging, Vol. 116, pp.6-15.
2. McDowell, D. L., Miller, M. P. and Brooks, D. C., (1994), "A Unified Creep-Plasticity Theory for Solder Alloys", Fatigue of Electronic Materials, ASTM STP 1153, pp.42-59.
3. Shine, M. C. and L. R. Fox, (1994), " Fatigue of Solder Joints in Surface Mount Devices", Low Cycle Fatigue, ASTM STP 942, pp. 588-610.
4. Frear, D. R., Burchett, S. N., Neilsen, M. K. and Stephens, J. J., (1997), " Microstructurally Based Finite Element Simulation of Solder JointBehaviour", Soldering & Surface Mount Technology, No.2, pp.39-42.
5. Lau, J. H. and Pao, Y. H., (1997), Solder Joint Reliability of BGA, CSP, Flip Chip, and Fine Pitch SMT Assemblies, McGraw-Hill.
6. Chow, C. L. and Wei, Y., (1996), "A Fatigue Model for Crack Propagation", Advances in Fatigue Lifetime Predictive Techniques, Vol.3, pp.86-99.
7. Chow, C. L. and Lu, T. L., (1989), " On Evolution Laws of Anisotropic Damage", Engineering Fracture Mechanics, Vol.34, pp.679-701.

* This work was supported by the United States Department of Energy under Contract DE-AC04-94AL85000. Sandia is a multiprogram laboratory operated by Sandia Corporation, a Lockheed Martin Company, for the United States Department of Energy.